Current Research in Food Science 8 (2024) 100780

Contents lists available at ScienceDirect

Current Research in Food Science

journal homepage: www.sciencedirect.com/journal/current-research-in-food-science

Effect of water content on gelatinization functionality of flour from sprouted sorghum

Miriam Chiodetti, Maria Grazia Tuccio, Eleonora Carini *

Department of Food and Drug, University of Parma, Parco Area delle Scienze, 47/A, 43124, Parma (PR), Italy

ARTICLE INFO

Handling Editor: Dr. Xing Chen

Keywords:
^{1}H NMR mobility
Drying treatment
Germination
Thermal properties
Hydration

ABSTRACT

Sorghum starch granules are encapsulated in a rigid protein matrix that prevents the granules from fully swelling and gelatinizing. Sprouting and subsequent drying treatment can affect the gelatinization properties of sorghum starch. This study aimed to evaluate the gelatinization properties of flours from unsprouted (US) and sprouted (S50, S40) sorghum dried at 50 °C (6h) and 40 °C (12h), respectively. Swelling power (Sp), thermal properties (DSC) and ^{1}H molecular mobility and dynamics were evaluated at different water contents (38–91%). Sp increased with increasing water content, with S40 showing the lowest values, probably due to prolonged amylase activity and thus starch breakdown. Sprouting increased gelatinization temperatures; however, these differences disappeared for high water contents (82 and 91%). From a molecular point of view, sprouted samples showed a decrease in protons associated to the rigid protein matrix and starch structures. ^{1}H CPMG results showed the presence of 4 populations at 38% water content. The evolution of the more mobile population with increasing water content supported the assignment of more mobile water fraction to this population. Sprouting decreased the mobility of populations in unheated samples, suggesting an increase in molecular bonds between flour biopolymers and water. After heating, however, increased molecular mobility in S40 indicated the formation of a weaker network between starch, protein, and water at the molecular level. These results suggest that post-sprouting drying treatment influences sorghum gelatinization, with potential modulation by water content. This study contributes to understanding the application of sprouted sorghum in foods with different moisture content.

1. Introduction

In recent years, the research interest about the use of sorghum (Sorghum bicolor (L.) Moench) in Western food products, has increased (Xiong et al., 2019; Rumler and Schönlechner, 2021; Rumler et al., 2022; Khoddami et al., 2023). Although sorghum is the fifth most grown cereal in the world (62.1 million tons annually produced and 41.7 million ha planted worldwide) (FAOSTAT, 2021), its use in food production has traditionally been limited to the semi-arid areas of the globe, such as Africa and Asia (Belton and Taylor, 2004; Dicko et al., 2006; Hariprasanna and Rakshit, 2016). In Western countries, sorghum has traditionally been destinated to animal feed (Khoddami et al., 2023). The growing interest in the use of sorghum is due to some interesting agronomic characteristics, for which it has been defined as a climate-resilient crop (Marchini et al., 2023). These factors include adaptation to a variety of agronomic and environmental conditions, such as low water requirements for cultivation and drought resistance (Xiong et al., 2019; Abdel-Ghany et al., 2020). Others peculiar factors are its nutritional properties, such as the absence of gluten (Ciacci et al., 2007; Pontieri et al., 2013) and the abundance of phenolic compounds, and its potential health benefits against obesity, cancer, and cardiovascular diseases. In this regard, we refer to numerous reviews published in recent years (de Morais Cardoso et al., 2017; Vanamala et al., 2018; Bean et al., 2019; Serna-Saldivar and Espinosa-Ramírez, 2019; Xiong et al., 2019; Rashwan et al., 2021; Espitia-Hernández et al., 2022; Khoddami et al., 2023).

Starch gelatinization widely contributes to the functionality of flours and their food applications (Goldstein et al., 2010; Zhu, 2014; Schirmer et al., 2015; Donmez et al., 2021). Indeed, when heated in the presence of excess water, the starch granules undergo a series of structural changes that are reflected from the molecular to the macroscopic level (Schirmer et al., 2015). First, the granules absorb water in the amorphous regions and swell, then water is absorbed by the crystalline regions, leading to the breakdown of amylopectin crystal structures and

* Corresponding author. Parco Area delle Scienze, 47/a, 43124, Parma, Italy.
E-mail addresses: miriam.chiodetti@unipr.it (M. Chiodetti), mariagrazia.tuccio@studenti.unipr.it (M.G. Tuccio), eleonora.carini@unipr.it (E. Carini).

https://doi.org/10.1016/j.crfs.2024.100780
Received 1 February 2024; Received in revised form 28 May 2024; Accepted 4 June 2024
Available online 6 June 2024

finally of the granule itself (Zhu, 2014; Donmez et al., 2021). Simultaneously with the melting of starch crystallites and the leaching out and solubilization of amylose, changes in physicochemical properties occur, such as the loss of birefringence and the increase in viscosity (Wang and Copeland, 2012; Zhu, 2014; Schirmer et al., 2015). The degree of starch gelatinization depends on several factors (heating rate, temperature, water content, presence of other components such as salts, sugars, proteins, lipids, non-starch polysaccharides) (Donmez et al., 2021). Among them, water content is of paramount importance; moreover, the interactions of other components of the food matrix both with water molecules and starch domain affect starch gelatinization (Wang and Copeland, 2012, 2013; Schirmer et al., 2015; Donmez et al., 2021). Usually, increasing levels of water favor high or complete gelatinization degree, increasing the DSC gelatinization enthalpy and granule swelling, and lowering the gelatinization temperatures (Wang and Copeland, 2012; Donmez et al., 2021). Different levels of gelatinization can influence food processing parameters and physico-chemical properties of final products (Schirmer et al., 2015). Therefore, to forecast the effects of starch gelatinization on food products and processes it is useful to investigate the gelatinization level and water dynamics in starchy products when different water contents are available.

Sorghum starch gelatinization has been reported to be characterized by higher transition temperatures than other grains (Serna-Saldivar and Espinosa-Ramírez, 2019). Moreover, the gelatinization of sorghum starch is limited due to protein-starch granule associations, proteins crosslinking and the presence of tannins. In particular, the presence of a strong protein matrix consisting of around 70% highly hydrophobic kafirins (Xiong et al., 2019), in which the granules are encapsulated, prevents the granules from fully swelling and gelatinizing (Taylor et al., 2006; Khoddami et al., 2023). On the basis of that, sprouting has been studied to modify and improve the nutritional, physicochemical and functional properties of sorghum (Rashwan et al., 2021). While sprouting has been reported to increase both the availability and digestibility of starch and protein, protein solubility, bioavailability of minerals and bioactive compounds, and to reduce the anti-nutritional compounds (Afify et al., 2011, 2012; Lemmens et al., 2019; Saithalavi et al., 2021), the technological properties of the starch fraction have been reported to worsen after sprouting (Li et al., 2017; Marchini et al., 2021b). Upon sprouting, the proteases and amylases of sorghum act reducing protein-starch interactions (Lemmens et al., 2019), but at the same time, amylases can breakdown starch granule structure, thus limiting the ability of the granules to gelatinize (Li et al., 2017; Lemmens et al., 2019). However, some studies have reported that post-sprouting drying conditions (Marchini et al., 2021b) and sprouting time and temperature (Singh et al., 2017; Cardone et al., 2021) tailor the effects of sprouting, including the technological functionality. In particular, the time-temperature combinations of the sprouting and post-sprouting drying treatments influence the degree of grain modification through the modulation of the enzyme activity (Singh et al., 2017; Cardone et al., 2021; Marchini et al., 2021b).

To the best of our knowledge, there are no studies focusing on the gelatinization properties of sprouted sorghum over a wide range of water contents. Such investigations have been carried out in the last 20 years for different starch sources, such as pea starch (Wang and Copeland, 2012), waxy corn, normal corn, potato and pea starches (Tananuwong and Reid, 2004), corn starch (Fu et al., 2014), potato dry matter and starch (Liu et al., 2002), and wheat starch (Orlowska and Randzio, 2010). The present study was undertaken to better understand the physicochemical properties and the gelatinization behavior of water-flour systems of sprouted and unsprouted sorghum flours. In particular, the role of water content (from 38 to 91%) in the thermal transitions of flour was studied to simulate the conditions of different moisture contents in foods. A combination of physico-chemical techniques, from the macroscopic to the molecular level, was used.

2. Materials and methods

2.1. Materials

White sorghum grains (Sorghum bicolor [L.] Moench) were soaked and sprouted at an industrial sprouting plant (Bühler AG, Uzwil, Switzerland) as reported in our previous study (Marchini et al., 2021a). The soaking and sprouting treatments were made under controlled temperature (25 °C) and relative humidity (90%), for 16 and 72 h, respectively. The post-sprouting drying treatments were chosen in order to compare the traditional sun drying conditions applied in some African countries (40 °C) (Elkhalifa and Bernhardt, 2010, 2013; Georget et al., 2012) and the temperature applied at an industrial level (50 °C) (Marengo et al., 2017; Marti et al., 2017). The drying time was set in order to obtain a comparable final moisture content of sorghum seeds (12.7 ± 0.0 g/100 g w.b.). After sprouting and drying, the sprouted grains (S50, S40), and the unsprouted control sample (US) were milled in order to obtain a whole grain flour with the following particle mass distribution: ≈23% of particles >300 μm; ≈30% of particles between 300 and 200 μm; ≈27% of particles between 200 and 100 μm; and ≈20% of particles <100 μm. Flour milling was performed with a laboratory mill (Labormill, BONA, Italy). For the proximate composition of above-mentioned flours, we refer to our previous study on the same flours (Marchini et al., 2021b).

2.2. Flour-water systems

Sorghum flour-water systems were prepared according to the water-flour ratio reported in Table 1 and considering the moisture content of flours. For simplicity, the water contents will be given below approximated to their respective integers. The hydration range was defined according to the hydration levels also reported in previous studies (Wang and Copeland, 2012; Schirmer et al., 2015), and representative of the conditions of low moisture foods and high moisture foods, in which starch is sufficiently or not sufficiently hydrated (Schirmer et al., 2015).

2.3. Swelling power (Sp)

The swelling power Sp of the samples was measured following the method described by Marchini et al. (2021b), with modifications. The water-flour systems were prepared in 2 mL Eppendorf tubes®, weighing the specific flour and distilled water, followed by vortex for 60 s. After that, the flour-water systems were heated in a water bath at 90 °C for 1 h. The samples were cooled to 30 °C for 30 min and centrifuged at 8000 rpm for 20 min. Once the supernatant was removed, the sediment was weighed. Sp was calculated as the ratio of sediment weight to the dry sample weight. Six replicates, divided in two different days, were carried out for each water-flour system.

2.4. Thermal properties

The thermal properties of water-flour systems were measured with a differential scanning calorimeter (DSC, Q200 TA Instruments, USA), calibrated with indium (melting point 156.6 °C, melting enthalpy 28.71 J/g) and mercury (melting point −38.8 °C, melting enthalpy 11.44 J/g).

Table 1
Water:flour ratio and moisture content of each sorghum water-flour system.

water:flour ratio (w:w)	moisture content (% d.b.)
0.42:1	38.0
1:1	56.0
2.3:1	73.3
4:1	82.4
9:1	91.2

Each water-flour system was prepared by placing the flour and distilled water, accurately weighed, into a stainless-steel pan (Perkin, USA). The system was gently stirred with a needle until it became homogeneous, taking care not to lose any of the sample. The pans were then hermetically sealed and kept at room temperature overnight before being analyzed. During the test, all the samples were equilibrated at 30 °C and then heated to 130 °C at 10 °C/min. An empty, hermetically sealed pan was used as a reference. Universal Analysis software (version 4.5 A, TA Instruments, USA) was used to determine the onset (T_{on}, °C), peak (T_{peak}, °C) and offset (T_{off}, °C) gelatinization temperatures and enthalpy change (ΔH, J g^{-1}) of each flow curve. At least 6 replicates, divided in two different days, were analyzed for each sample.

2.5. Proton molecular mobility

The ^{1}H molecular mobility of water-flour systems was analyzed through a low-resolution nuclear magnetic resonance (NMR) spectrometer (Minispec, Bruker, Massachusetts, USA) with a frequency of 20 MHz. Samples were prepared by weighing 1 g of flour and different amounts of water in NMR tubes (10 mm diameter), according to the water-flour ratio reported in Table 1. After that, samples were mixed with a small spatula and then vortexed for 60 s. To compare the non-gelatinized and the gelatinized samples, each water-flour suspension was analyzed raw (unheated) and after heating (90 °C; 1 h) and cooling (30 °C; 30 min). All the NMR tubes were sealed with Parafilm® to prevent water loss during heating, cooling and during the analysis.

^{1}H Free Induction Decay (FID) and Carr-Purcel-Meiboom-Gill (CPMG) pulse sequences were used to analyze the sample molecular mobility. During the analysis the temperature was set at 25.0 ± 0.1 °C using an external thermostatic bath (Julabo F30, Julabo Labortechnik GmbH, Seelbach, Germany).

The ^{1}H FID curves were acquired to measure the mobilities and abundances of the least mobile proton populations detectable in the molecular time-frame window of the instrument used (7–500 μs). The experiment was performed with 32 scans and 900 data points, with a single 90° pulse, followed by a dwell time of 7 μs, a recycle delay of 1 s, and an acquisition window of 0.5 ms. To quantitatively obtain the proton relaxation times and relative abundances of each population, ^{1}H FID curves were fit with a two-component model (exponential and Gaussian; Le Grand et al., 2007). The fit was performed with Sigmaplot software, v.10 (Systat Software Inc., USA) according to the following equation [1]:

$$f(t) = y_0 + A^* e^{\left(\frac{t}{TA}\right)} + B^* e^{\left(-\frac{t}{TB}\right)^2} \quad \text{(Eq. 1)}$$

Where y_0 is the FID decay offset, A and B are the intensities of each relaxation component, and TA and TB are the apparent relaxation times.

The Carr-Purcel-Meiboom-Gill pulse sequence (Meiboom and Gill, 1958) was used to measure the ^{1}H T_2 relaxation times of more mobile protons than those observed in the ^{1}H FID window. The experiment was performed with 32 scans, a recycle delay (RD) of 1 s, an interpulse spacing (τ) of 0.04 μs and 2500 data points. The ^{1}H CPMG curves were analyzed as quasi-continuous distributions of relaxation times using UpenWin software (Alma Mater Studiorum, Bologna, Italy; Borgia et al., 1998, 2000). Default values were used for all UPEN parameters, except for the LoXtrap parameter, which was set = 1 to avoid extrapolation of relaxation times shorter than the first experimental point.

Four tubes, divided in two different days, were analyzed for each water-flour system, and two ^{1}H FID and ^{1}H CPMG acquisitions were taken from each tube. In total, eight ^{1}H FID and eight ^{1}H CPMG curves were analyzed for each water-flour system.

2.6. Statistical analysis

The data collected were analyzed by one-way analysis of variance (ANOVA) at a significance level of 0.05, followed by Tukey, LSD and Games Howell *post-hoc* tests, according to the homogeneity of sample size and homogeneity of variance among the groups (SPSS software v.27, IBM SPSS Inc., Chicago, IL, USA).

3. Results and discussion

3.1. Swelling power

In this study, the gelatinization capacity of three different types of sorghum flour, unsprouted (US), sprouted and dried at two different temperatures (S40 and S50), was evaluated at five different water contents. As described above, the gelatinization capacity of starch is influenced by the water content available in the matrix. In fact, the amount of available water that is absorbed by the granule when heated contributes to the degree of gelatinization itself. Swelling power represents one of the parameters by which the gelatinization degree of a starch or flour can be assessed. The absorption of water and the resulting loss of molecular order in the amorphous and crystalline regions of the granules result in the swelling of the granules (Wang and Copeland, 2012, 2013).

During the Sp analysis, no supernatant was formed after the centrifugation process in the samples with a water content of less than 73%. This indicates that all the added water was completely absorbed by the flour and no amylose leaching occurred (Wang and Copeland, 2012). With water contents ≥73%, the samples showed the formation of supernatant. This shows that up to 73% water content the system was in a water-limited condition, whereas following higher water addition the samples were able to absorb more water until the starch polymers began to leach. The Sp results obtained from the analysis of the different water-flour systems are shown in Fig. 1. As can be observed from the graph and easily assumed, the swelling power of the samples was found to increase as the water content increased ($p < 0.05$ in all samples at all water contents). Specifically, going from 38 to 91% of water, the swelling power of US sample showed an increase of ~+390%, the sprouted and 50 °C dried sample (S50) of ~+181%, and the sprouted and 40 °C dried sample (S40) of ~+152%. The increase in Sp with increasing water content is mainly determined by the swelling capacity of highly branched amylopectin. In fact, while linear amylose swells and then dissolves in water, amylopectin swells and is not lost (Wang and Copeland, 2012). The increase in Sp as a result of increased water content has been demonstrated by previous studies on starch or flour

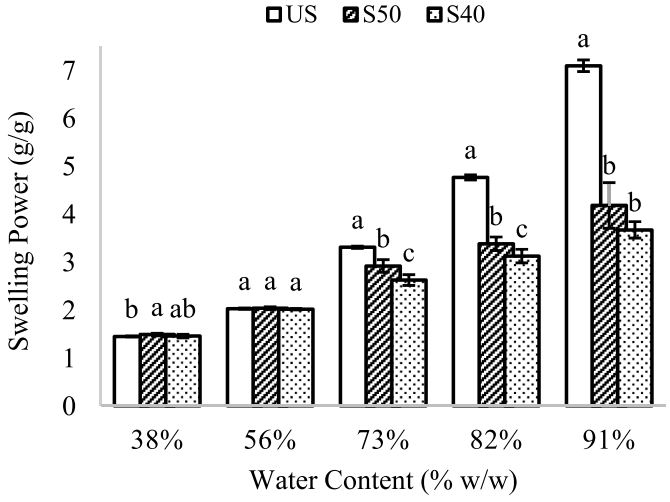

Fig. 1. Swelling power of US (flour from unsprouted sorghum), S50 (flour from sprouted and 50 °C dried sorghum) and S40 (flour from sprouted and 40 °C dried sorghum) samples at 38, 56, 73, 82, and 91% water contents. Different lowercase letters indicate significant differences between US, S50 and S40 at the same water content ($p < 0.05$).

(Wang and Copeland, 2012; Wang et al., 2014).

Regarding the effect of sprouting and drying treatments on sorghum flour swelling power, the results showed that the Sp in the sprouted samples decreased after sprouting treatment. In fact, as can be seen from Fig. 1, the swelling power of US sample resulted higher than that of sprouted samples from 73% water content. The difference between sprouted and unsprouted samples increased with increasing water content. Indeed, the largest difference was found at the highest water content (91%). This indicates that, after heating and cooling, US sample showed a higher increasing ability to retain water with water content increase, if compared to sprouted samples. This may be due to the fact that sprouted samples had a higher amylose content and therefore, proportionally, less amylopectin than US sample [the amylose content and proximate composition of flours are reported in Marchini et al. (2021b)]. Indeed, many studies have reported that a higher amylose content and a lower amylopectin content negatively influences the swelling of granules and thus the swelling power (Li and Yeh, 2001; Wang et al., 2014). Elkhalifa and Bernhardt (2013) also found that sorghum flour sprouted and dried at 40 °C showed a decrease in swelling power compared with unsprouted sorghum flour (Sp at 85 and 100 °C). This effect was intensified in Sp at 100 °C by increasing the sprouting time. Cardone et al. (2021) also reported that sprouting for 96 h (dried at 50 °C × 9h) significantly reduced Sp of sorghum flour. These authors explained this result as a consequence of the degradation of sorghum protein bodies that occurred during germination, which made the starch more available for gelatinization but also more susceptible to α-amylase attacks. However, under conditions of limited amount of water (38% and 56%) the differences among the three samples appeared to taper off. Specifically, at a water content of 56%, the average values of the three samples were comparable indicating that the samples retained the same water as a result of gelatinization process, while, at the lowest water content (38%) the Sp value of S50 was higher than US, but not significantly different to S40. This could be related to the lower or absent leaching of amylose at low water contents, since, as discussed above, no supernatant formation was seen under 73% water content. Another reason could be an increased starch availability as a result of protein matrix breakdown that occurred upon sprouting, that may be more evident at low water contents.

Comparing the two sprouted samples, it was seen that S50 showed higher Sp than S40 for 73% and 82% water contents. This is indicative of higher starch swelling power when sprouted sorghum is dried at 50 °C. The differences highlighted how the drying phase may be of relevance in determining the functionality of sprouted grains. These data could support the hypothesis that greater starch destructuring results in less water retention during gelatinization.

3.2. Thermal properties

Based on DSC analysis, a main endothermic peak between ~65 and ~99 °C was identified. This peak has been associated with the breakdown of starch crystalline order (or double-helix structures) that occurs during starch gelatinization (Goldstein et al., 2010). A second endothermic peak between ~96 and ~125 °C was also identified in some thermograms (Fig. S1) and associated to the melting of amylose-lipid complexes (Zhu, 2014). The heating rate used (10 °C/min) may have reduced the resolution of this second minor peak and for this reason, it was not further considered for analysis and discussion in this work. Fig. 2 shows the thermograms of the three samples, for each water content, and Table 2 the transition enthalpy and temperatures.

The main endothermic peak, related to the melting of starch granules, was found to increase with increasing water content, in all samples. The dependence of this endothermic peak on water content is reported by numerous studies (Liu et al., 2002; Goldstein et al., 2010; Wang and Copeland, 2012; Wang et al., 2014). Regarding the onset and end-transition temperatures associated to the main endothermic peak (T_{on} and T_{off}), they were found to generally decrease with increasing water content (Table 2). Specifically, in the sprouted S50 and S40 samples, the entire peak shifted to lower temperatures, resulting in decreasing T_{on}, T_{peak}, and T_{off} values. Instead, only the T_{peak} and T_{off} values decreased with increasing water contents in US, indicating that the range of gelatinization temperatures in sprouted samples remained almost constant, while in the unsprouted decreased. Goldstein et al. (2010) and Liu et al. (2002) also associated higher temperatures with low water contents. In fact, at low water contents the granules are not fully hydrated and remain structured, requiring more heat energy for dissociation. In general, the effect of water content on gelatinization temperatures was more pronounced in sprouted samples than in unsprouted samples. In fact, from 38 to 91% water content, the T_{peak} decreased by about 10 °C in the sprouted samples, and by about 4 °C in the US (Table 2). The T_{on} of US sample also did not change by increasing the water content. This means that varying water content is more crucial in determining flour functionality (in terms of gelatinization temperatures) in sprouted sorghum than in unsprouted sorghum.

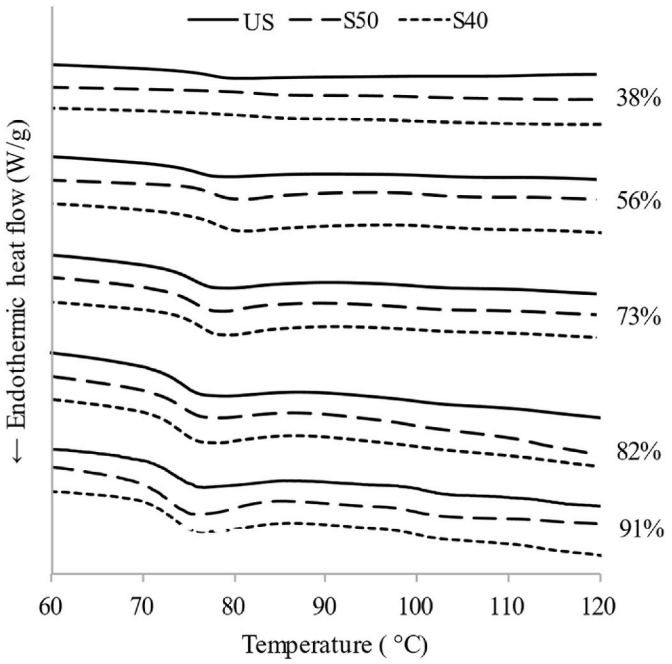

Fig. 2. Representative DSC thermograms of US (flour from unsprouted sorghum), S50 (flour from sprouted and 50 °C dried sorghum) and S40 (flour from sprouted and 40 °C dried sorghum) samples at different water contents.

S50 and S40 samples tended to show higher gelatinization temperatures than the US sample (Table 2). These differences emerged clearly at low water contents, while they almost disappeared at high water contents. The reason could be that sprouted samples had higher amylose contents than US [29 ± 3% (US), 34 ± 4% (S50), 47 ± 0% (S40) (Marchini et al., 2021b);]. Several studies reported that gelatinization temperatures of starches with high amylose content are generally higher than those with less amylose content (Wu et al., 2013; Wang et al., 2014). However, there is no shortage of studies reporting instead that the presence of long chain amylopectin forming complex crystal structures requires more energy, and thus heat, to dissociate (Lin et al., 2016; Zhang et al., 2020). In addition, it has been reported that even the presence of sugars can increase the gelatinization temperatures, thus possibly explaining higher temperatures in sprouted samples (Wu et al., 2013). Interestingly, at high water contents (82 and 91%), when the samples were more hydrated, differences between samples disappeared, and the gelatinization temperatures resulted the same between US, S50 and S40 (Table 2). Therefore, when the samples are granted abundant hydration, the loss of molecular order occurs at the same temperatures. This is an interesting result in limiting the effect of increasing

Table 2
Thermal properties of US (flour from unsprouted sorghum), S50 (flour from sprouted and 50 °C dried sorghum) and S40 (flour from sprouted and 40 °C dried sorghum) samples. Different lowercase letters indicate significant differences between US, S50 and S40 at the same water content ($p < 0.05$). Different capital letters indicate significant differences between 38, 56, 73, 82, and 91% water contents at equal flour used ($p < 0.05$).

	Water content	Sample name		
		US	S50	S40
ΔH (J/g)	*38%*	3.76 ± 0.29 aD	1.06 ± 0.48 bC	0.99 ± 0.11 bC
	56%	4.63 ± 0.60 bC	4.42 ± 0.41 bB	6.05 ± 0.40 aB
	73%	6.38 ± 0.50 aB	6.64 ± 0.61 aA	5.83 ± 0.88 aB
	82%	7.73 ± 0.27 aA	6.93 ± 0.89 aA	6.23 ± 1.21 aAB
	91%	6.90 ± 1.08 aB	6.12 ± 1.73 aAB	8.12 ± 1.08 aA
T_{on} (°C)	*38%*	67.00 ± 0.98 bAB	74.10 ± 1.17 aA	73.01 ± 1.02 aA
	56%	65.69 ± 1.57 bCB	71.05 ± 1.65 aB	69.22 ± 1.72 aB
	73%	66.44 ± 1.21 bCB	66.11 ± 0.93 bC	69.82 ± 0.59 aB
	82%	65.27 ± 1.15 bC	67.24 ± 0.13 aC	68.77 ± 1.17 aB
	91%	68.37 ± 1.23 bA	66.94 ± 0.80 aC	69.02 ± 0.40 aB
T_{peak} (°C)	*38%*	79.19 ± 0.63 bA	84.59 ± 0.86 aA	85.40 ± 0.64 aA
	56%	78.44 ± 0.75 bAB	79.52 ± 1.41 aB	80.28 ± 0.65 aB
	73%	77.44 ± 0.28 aB	78.10 ± 0.66 aC	78.01 ± 0.52 aC
	82%	76.78 ± 0.24 aC	76.80 ± 0.24 aD	77.00 ± 0.42 aD
	91%	75.64 ± 0.47 aD	75.28 ± 0.39 aE	75.57 ± 0.37 aE
T_{off} (°C)	*38%*	97.87 ± 1.38 aA	98.90 ± 1.15 aA	97.69 ± 0.23 aA
	56%	97.40 ± 1.27 aA	98.08 ± 2.49 aA	98.21 ± 1.47 aA
	73%	90.67 ± 1.22 bB	94.59 ± 1.17 aB	89.48 ± 1.37 bB
	82%	90.93 ± 0.99 aB	90.82 ± 1.28 aC	89.35 ± 1.59 aB
	91%	87.20 ± 0.97 aC	86.60 ± 1.42 aD	87.05 ± 1.07 aC

gelatinization temperatures in sprouted grains.

As reported in Table 2, the ΔH of US and S50 reached its maximum value at a water content of 82%, and then began to decrease slightly. The ΔH of S40, on the other hand, continued to increase after the addition of a higher water content (91%). This phenomenon indicates that, by increasing the water content to the 82% level, maximum gelatinization occurred in US and S50. Similar behavior was observed, even if at different water contents, by Liu et al. (2002) on potato dry matter endotherms. It is worth noting that, although changes in ΔH can be attributed to starch modifications in sorghum flour, other components present in the flour (nonstarch polysaccharides, proteins, lipids, minerals) can affect the ability of starch to gelatinize (Liu et al., 2002; Donmez et al., 2021). In fact, the presence of protein bodies and the hydrophobic nature of sorghum protein matrix, in which starch is trapped, are known to have a limiting effect on starch gelatinization (de Mesa-Stonestreet et al., 2010; Cardone et al., 2021). In sprouted samples, the negative effect of proteins and lipids on starch gelatinization may have been modulated by the enzymatic hydrolysis that proteins and lipids underwent during sprouting. The more prolonged enzyme activity during the drying treatment in S40 might have shown a more pronounced change in protein ability to hinder starch functionality, and thus allowing it to increase the degree of gelatinization even for water contents higher than 82%. These results contrasted with those found for swelling power, where the sample continued to swell even after the water content exceeded 82%. In addition, even when comparing the values of ΔH between US, S40 and S50, they were found to contrast with swelling power results. In fact, Sp analysis showed generally higher values in US sample than S40 e S50, suggesting better gelatinization properties in US than sprouted samples. The enthalpy change, however, did not show the same trend. By contrast, ΔH resulted higher in US only at 38% water content, while it was higher in S40 at 56% water content and no significant differences were found at other water contents. As reported above, S40 was the sample that exhibited the most pronounced effect of the sprouting treatment on swelling power and ΔH, probably due to more prolonged enzyme activity during drying treatment. In the case of swelling power, however, it worsened, while in the case of ΔH, it partially improved. It should be kept in mind that, in this study, swelling power was calculated as the weight difference related to the retained water after heating, cooling, and removal of supernatant; ΔH, on the other hand, symbolizes the loss of molecular order in the granule structures over a temperature ramp and could provide slightly different information than swelling power. In addition, if the ΔH gelatinization results refer to the specific starch transition, in the case of swelling power the effect of proteins and their ability to bind water and form a gel upon cooling might have influenced the result of Sp.

3.3. Proton molecular mobility

^{1}H FID experiments. The ^{1}H FID analysis of unheated and heated water-flour systems showed the presence of two ^{1}H populations A and B, giving 100% of the total ^{1}H FID signal. The relaxation times and relative abundances of Pop A and Pop B of heated and unheated samples at all water contents are given in Table S2. ^{1}H FID populations of unheated samples relaxed in the range of 0.0133–0.0149 ms (Pop A) and 0.3506–0.8295 ms (Pop B). These findings agree with those previously reported on sorghum flour (Marchini et al., 2021a). Indeed, ^{1}H FID analysis shows the most rigid proton populations with least water contact in water-flour systems. In particular, in unheated systems, the most rigid Pop A has been assigned to the rigid CH protons of crystalline and amorphous structures not in contact with water and of proteins in strong interaction with each other (hydrophobic parts and regions with protein-protein interactions) (Bosmans et al., 2012) which can be reasonably related to the crosslinking of sorghum proteins. On the other hand, the more mobile Pop B has been assigned to the CH protons of amorphous starch and proteins in little contact with confined water (Bosmans et al., 2012). After heating, ^{1}H FID populations showed relaxation times in the range of 0.0161–0.0195 ms for Pop A and 0.2966–0.8587 for Pop B. Fig. 3 reported the Pop A (%) evolution as a function of water content and heating treatment in US, S50 and S40 samples. After heating, the ratio of Pop A (%) to Pop B (%) in the samples changed, marking a decrease in abundance of Pop A and an increase in abundance of Pop B, if compared to unheated samples (Fig. 3; Table S2). The decrease in Pop A (%) after heating indicates the melting of the crystalline and amorphous structures packed in the starch granules, which occurred during gelatinization. However, the lasting presence of Pop A after heating has been reported to indicate the presence of amorphous structures that remained immobile after heating and the neoformation of amylose crystals after cooling (Bosmans et al., 2012). A decrease in the first population upon heating was also reported by Rondeau-Mouro et al. (2015) in wheat starch models and dough at ~45 % water content. These authors stated that this first component represents a fraction of protons potentially transferable to the other components. In fact, in addition to protons from amylopectin, this population may represent protons from well-organized amylose structures that transfer to the higher mobility population and to the extragranular water phase during amylose leaching that occurs in the swelling process

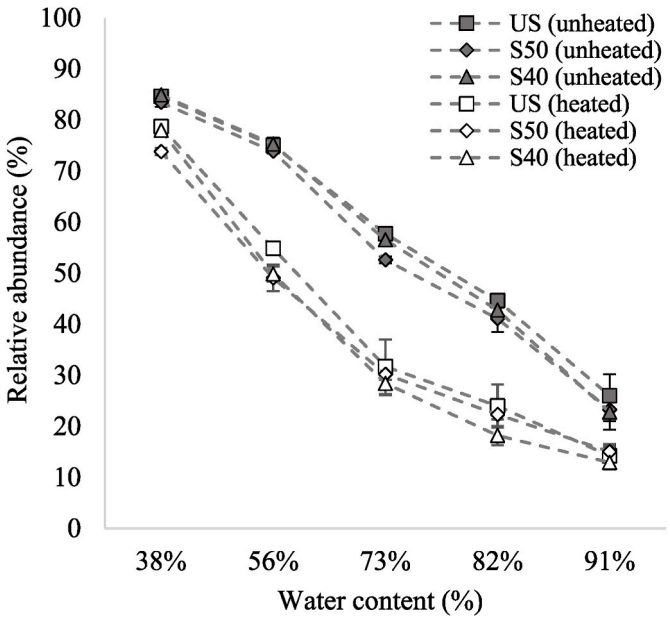

Fig. 3. Evolution of Pop A (%) with increasing water content in unheated and heated water-flour systems.

(Rondeau-Mouro et al., 2015; Rakhshi et al., 2022). As can be observed from Fig. 3, the decrease of Pop A (%) abundance from unheated to heated systems, resulted to be dependent on water content, indicating the greatest differences at 56, 73 and 82% water content. At 38% water content, gelatinization of the samples may have not been completed due to limited water content, thus leading to the prevalence of more rigid starch structures even after heating and cooling. At 91%, the high water content markedly reduced the Pop A (%) signal in unheated systems (if compared to lower hydration levels), while in the gelatinized samples the signal decreased to a lesser extent, probably because gelatinization was almost already completed at 82% water content.

Generally, in both unheated and heated samples, the percentage of Pop A decreased (and thus Pop B increased) as water content increased. Probably, in unheated samples, the increasing water content facilitated the water uptake into flour structures, leading to an increase in protons in little contact with water and a decrease of fraction not in contact with water. These results were also found by other authors (Marchini et al., 2021a; Parenti et al., 2021). In heated samples, on the other hand, the decrease of pop A with water increase, can be linked to the extent of starch gelatinization that occurred in water-flour systems. A higher water content can generally be linked to a higher gelatinization, and thus a higher decrease in rigid starch structures. Looking at the mobility of pop A, in the unheated samples, tA tended to increase with increasing water content, while no trend was observed in heated samples. These data highlight the effect of water entry in the channels between the stiffer starch structures in the unheated samples. Instead, a more similar and homogeneous structure in the domain representing the pop A of heated samples at different water contents can be hypothesized. The presence of water in these very constrained zones was also reported by Rondeau-Mouro et al. (2015).

Comparing the three flour samples, S50 showed lower Pop A (%) values than US in unheated systems for all water contents, while S40 resulted higher than US only from 73% water content onward (Fig. 3, Table S2). The lower Pop A (%) values in sprouted samples compared to US, may be associated to the breakdown of sorghum rigid protein matrix and modification of starch structures mediated by enzyme hydrolytic activity that occurred during sprouting. These modifications of sorghum matrices may have led to an increase in the signal of the population in little contact with water, assigned to Pop B. Even after heating, the sprouted samples (S40, S50) tended to show lower values of Pop A (%) than US sample. This effect, however, was not consistent at all water levels (Fig. 3; Table S2). Lower Pop A (%) values in heated sprouted samples than US could be due to a different degree of gelatinization of amylopectin crystals and amorphous starch as an effect of sprouting. Another finding to note is the tendency for greater mobility of Pop B in both unheated and heated samples after sprouting (S40 and S50) (Table S2), which may be related to the general breakdown of structures that occurred upon sprouting.

CPMG experiments. The CPMG analysis of unheated samples (US, S40 and S50) at 38% water content revealed the presence of 4 ^{1}H T_2 populations, named Pop C, D, E and F, respectively (ascending order of mobility; Fig. 4). This result agrees with previous findings on water-sorghum flour systems (Marchini et al., 2021a). According to the

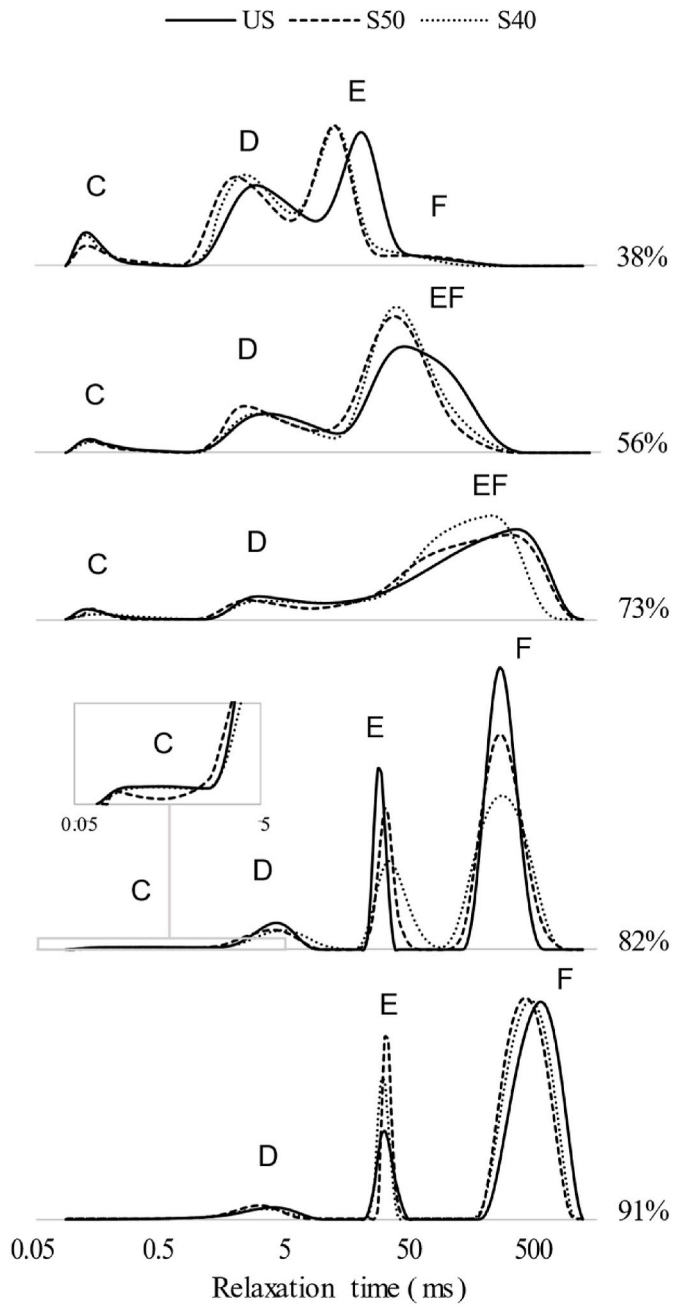

Fig. 4. Evolution of representative ^{1}H T_2 CPMG populations of unheated US (flour from unsprouted sorghum), S50 (flour from sprouted and 50 °C dried sorghum) and S40 (flour from sprouted and 40 °C dried sorghum) samples at different water contents.

literature, the 4 populations can be attributed to CH protons of amorphous starch and proteins in little contact with water and dietary fiber constituents (Pop C); to OH protons of intragranular water and starch, and CH protons of proteins in interaction with confined water (Pop D); and to the exchanging extragranular protons of bran and flour biopolymers in interaction with water (Pop E) (Bosmans et al., 2012; Marchini et al., 2021a). The most mobile Pop F has been attributed to both weakly water-bound OH protons (Marchini et al., 2021a; Parenti et al., 2021) and the lipid fraction of flour (Assifaoui et al., 2006; Hager et al., 2014). In our study, some considerations need to be made. At 38% water content, the protons of two main CPMG populations were represented by those related to exchanging protons of water and intra- and extra-granular starch structures and those of proteins in exchange with confined water or in strong interaction with water (Pop D and E); at the same time, a very small contribution of protons related to Pop F was denoted (Fig. 4). Moving from 38% to higher values of water content, the number of populations of unheated samples decreased to 3 populations. Specifically, at 56 and 73% water content, the populations E and F converged into a single new population (Pop EF), given by the merger of the two, which had intermediate relaxation times between these populations (Fig. 4). Moving from 56% to 73% water, the mobility of Pop EF increased with increasing water content. Interestingly, for water contents $\geq$82%, a new separation of Pop EF occurred, allowing the distinction of Pop E and Pop F. According to Ruan et al. (1999), when all water-binding sites in the flour are saturated, further addition of water forms new, more mobile water layers with increasing distance to water molecules bound to the flour solids (Ruan et al., 1999; Riley et al., 2022). Pop F would then show a progressive increase given the increase in water content, becoming the main population at water contents of 82 and 91%. The dynamics of Pop F evolution can be explained by the results of Le Botlan et al. (1998), which reported that water contents just above the appearance threshold of "weakly bound" water form a new layer that has a low degree of freedom due to physical reasons that prevent it from rapidly exchanging with the molecules of the "bound" water layers. This water, therefore, has slightly longer relaxation times than "bound" water (Le Botlan et al., 1998) and could explain the lack of complete peak resolution down to a 73% water level in our study. Le Botlan et al. (1998) also reported that when the water content increases, water molecules may begin to exchange with new water molecules in their surroundings and thus acquire greater mobility. This phenomenon could explain the subsequent resolution of the two populations E and F with water contents of 82 and 91%. These data could therefore support that Pop F consists of OH protons of weakly bound water, as reported by other previous studies (Parenti et al., 2021). The more rigid Pop C and Pop D gradually decreased with increasing water content. Population C seemed then to disappear at water contents >82% (Fig. 4). Presumably, the relative signal attributable to Pop C became too small compared to the high-mobility components. However, the mobility of Pop C and D was not affected by water content. This behavior is reasonable considering that Pop C and D belong to flour fractions less in contact with water. In contrast, the mobility of Pop E and F was found to be strongly affected by water content. This result agrees with what has already been reported by other authors (Le Botlan et al., 1998; Tananuwong and Reid, 2004; Riley et al., 2022), who stated that proton mobility of starchy products is directly related to water content, especially in case of fractions with high proton mobility, which in this case could be represented by Pop E and F.

Regarding the molecular differences between US, S40 and S50, different proton relaxation times were observed. Indeed, up to 73% water content, a higher mobility of the D, E and F (or EF) populations was found in the US sample than in the sprouted samples (Fig. 4), while at 82% population E was more rigid in US. The general lower mobility in sprouted samples can be explained by the presence of a higher number of bonds established with water within different structural domains of starch and protein. Indeed, sprouting may have led to a greater exposure of biopolymers binding sites as a consequence of the hydrolysis that occurred upon sprouting. The modification of the properties of starch and protein occurring during sprouting, may explain the differences found in the population mobility. In this regard, it was reported that the degradation of amylopectin chains reduces crystalline areas by facilitating water access in the granules (Jakobi et al., 2018), while other authors reported an increased ability of proteins to bind water after sprouting (Elkhalifa and Bernhardt, 2010; Lemmens et al., 2019; Marchini et al., 2021a). However, Rakhshi et al. (2024) found that the heat-induced transformation of model dough systems matched that of their starch-water system counterparts, highlighting how these differences are mainly due to starch properties. The main effect of starch on T_2 relaxation was also reported by Riley et al. (2022). However, Rakhshi et al. (2024) also reported that proteins may also have an impeding effect on starch-water interactions. Sprouting treatment may have changed this hindering effect of proteins and thus the starch-water interactions.

Heating and subsequent cooling of US, S40 and S50 changed the ^{1}H CPMG relaxation times distribution of the samples. Fig. 5 shows the comparison between the unheated and heated US sample, by way of example. In all samples, a decrease in mobility of Pop E and Pop D after heating and cooling was observed. In fact, during heating, the process of gelatinization occurred, which includes the entry of water, swelling and rupture of starch granules with the melting of crystal structures and mobilization of amylose outside the granules. This in turn may have led to a redistribution of protons characterizing the different populations at the molecular level. Moreover, after cooling, the subsequent gel formation resulted in the decrease of the relaxation times of the extragranular exchanging protons of flour biopolymers interacting with water (Pop E), and in the marked decrease in the abundance of protons with intragranular bonds between water and starch, as well as of the proteins in contact with the confined water (Pop D). The differences in the mobility of Pop D between heated and unheated systems appeared reasonably more pronounced at low water contents (38 and 56%), as insufficient water was available in unheated systems to allow the granules to break and swell. Rondeau-Mouro et al. (2015) reported that the decrease during heating of intragranular protons in starch model systems at ~45% water content was related to granule disintegration and viscosity improvement phenomena. At 56 and 73% water content, a decrease in mobility of Pop E (or EF) was observed. A decreased mobility of Pop E after heating and cooling was also reported by Bosmans et al. (2012) and Hager et al. (2014) in water-flour systems, where the water content was 47%. Furthermore, in heated systems Pop C disappeared at a lower water level than in the unheated systems. In fact, in heated systems, it was no longer observable from a water content of 82%, while, at 73%, it overlapped with Pop D. This indicates that increasing water content and heating led to a gradual and progressive reduction of CH protons of starch and proteins in little contact with confined water in the sheets, in favor of the high mobility populations in the continuous network between starch, protein and water. In heated systems with a water content of 82%, although two populations (E and F) were visible, they were not fully resolved. Indeed, unlike the unheated systems, where complete separation and resolution of E and F populations occurred at 82%, in the heated systems complete separation of E and F populations occurred at 91% water content. This result indicates the presence of an exchange between weakly bound water molecules and the starch-protein-water network at higher water content levels than in unheated systems. At 91 % water content, the most represented population was Pop F, attributed to the protons of more mobile and weakly bound water expelled from the starch-protein-water network.

Comparing the results of Pop B (FID) with those of Pop C (CPMG), in our work an exact correspondence between the two populations was not found. Pop B was found to increase up to the maximum water content analyzed, while Pop C was found to decrease until it disappeared with increasing water content, both in heated and unheated systems. This result differs from other previous studies, in which these two populations were associated with the same protons, as they relaxed at the

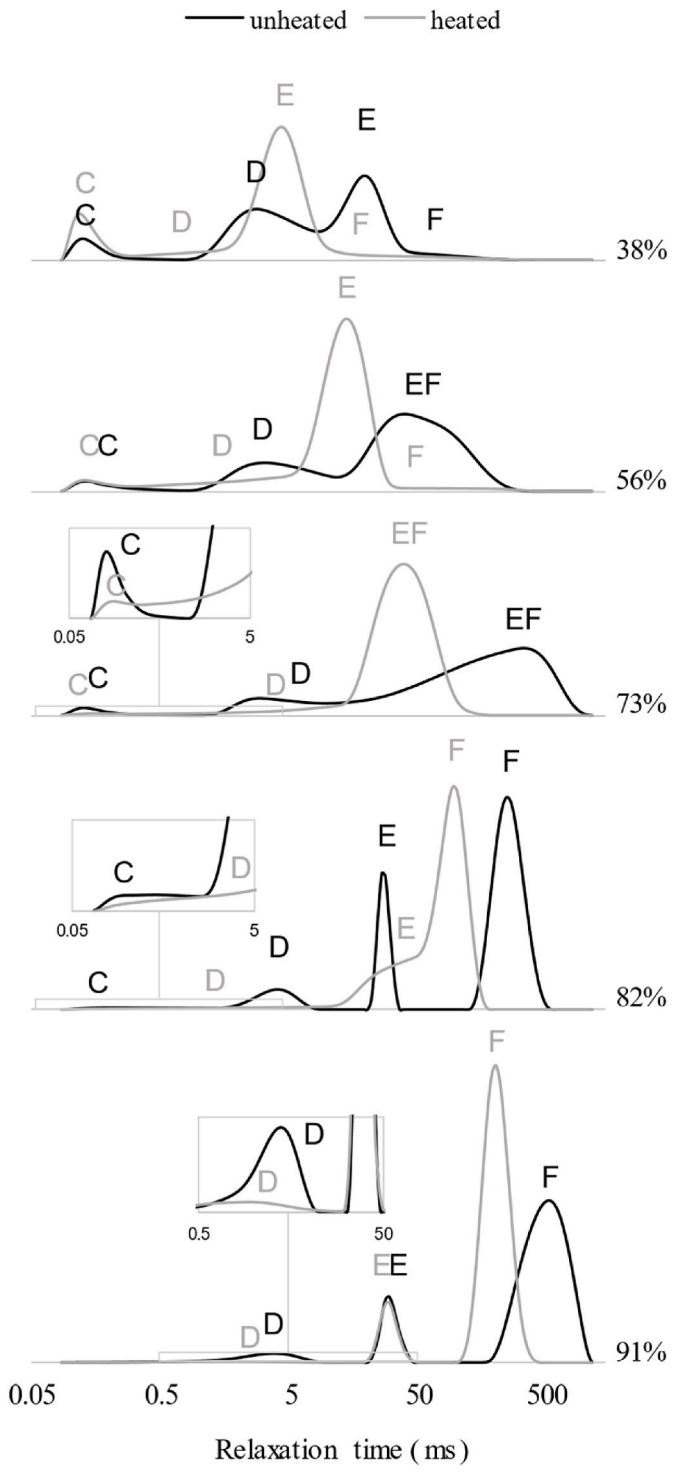

Fig. 5. Comparison of representative ^{1}H T_2 CPMG populations of unheated and heated US sample at different water contents.

same times and had similar behavior before and after heating (Bosmans et al., 2012; Riley et al., 2022). In the cited studies, however, Pop B and C were not evaluated at different water contents. Furthermore, it must be considered that Pop B and C are determined by two different RF sequences, in which proton mobility is assessed at different scales and the relative signal of the populations is returned independently. In fact, the two sequences provide relative, not absolute, data. Compared with low-mobility populations determined by FID analysis, the relative percent signal of Pop B increases with increasing water content because the signal of A decreases, and together they return 100 % of the total FID signal. In the CPMG experiment, on the other hand, Pop C is the more rigid population, whose relative contribution, compared with those with higher mobility, decreases as water content increases.

Looking at the comparison between sprouted samples with the unsprouted samples after heating and cooling (Fig. 6), Pop C in the sprouted samples (S40, S50) showed lower relative abundance than in the US. This indicates a post-heating less permanence of the rigid structures in the sprouted than in the unsprouted, due to the hydrolysis of starch and protein operated by enzymes during sprouting.

As for the higher mobility populations, however, the mobility of pops E and F (or EF) of sample S40 was higher than that of US and S50 (Fig. 6). US and S50, on the other hand, showed similar mobilities. This indicates the presence of weaker and more mobile bonds between water and biopolymers after heating in S40. As previously reported in other studies, this event could be due to the hydrolytic breakdown operated by amylases on starch, which caused a reduction in the swelling power of the sprouted samples (Marchini et al., 2021b). In addition, it may also be related to the different ability of proteins to form a gel of different strength in the newly formed continuous network. At a macroscopical level, a lower gel consistency in sprouted samples was reported by Singh et al. (2017).

4. Conclusions

In this study, we evaluated the effect of water content and different post-sprouting drying conditions (40 °C for 12h; 50 °C for 6h) on the macroscopic (swelling power), mesoscopic (thermal properties by DSC) and molecular properties (^{1}H molecular mobility and dynamics by LR ^{1}H NMR) of sorghum flour.

Sprouting and subsequent drying treatment affected all the analyzed properties. The swelling power of the samples was found to be compromised after sprouting at high water contents (≥73%), probably due to the negative effect of the enzyme activity on the ability of amylopectin to swell during gelatinization, but also to changes in the functionality of sorghum proteins. However, low-medium water content proved to be a promising condition for the functionality of sprouted flours, as the swelling power was equal or higher in sprouted than unsprouted. The swelling power of the sample dried at 40 °C was the most affected by sprouting treatment. Prolonged enzyme activity may have led to excessive destructuring of starch, making it more accessible but compromising some functional properties. However, as a result of sprouting, sorghum starch resulted more accessible and available to gelatinize, showing higher ΔH values in DSC results. In particular, at medium water content, the gelatinization enthalpy was higher in sprouted grains than unsprouted. The molecular properties of sorghum

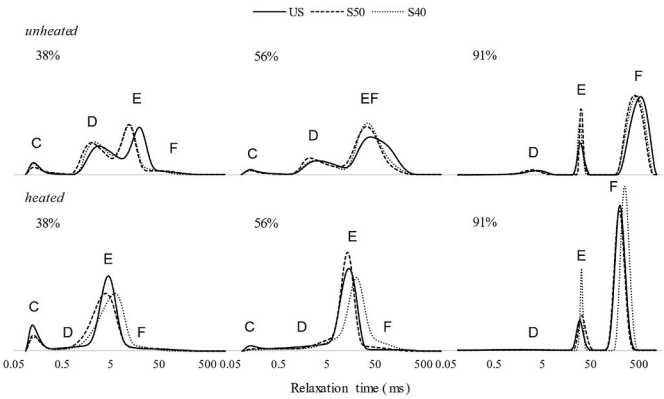

Fig. 6. Comparison of representative 1H T2 CPMG populations of unheated and heated US (flour from unsprouted sorghum), S50 (flour from sprouted and 50 °C dried sorghum) and S40 (flour from sprouted and 40 °C dried sorghum) samples at selected water content (38, 56 and 91%).

flour were also affected by sprouting and drying treatment, showing the reduction of the abundances of the most rigid populations in favor of those with higher mobility. The highest mobility of the population related to starch and protein protons in strong interaction with water (after heating and cooling) in the sprouted sample dried at 40 °C for 12 h revealed the presence of weaker bonds in the network formed. In general, in all the analysis performed, the sample dried at 40 °C for 12h was the one with the values that differed the most from the unsprouted sample, probably due to a more prolonged enzyme activity during the drying phase.

These results may be important when considering the potential application of sprouted sorghum flour in foods with different moisture contents, which help to understand how to improve the use of this flour in Western food products, improving the nutritional profile but without compromising technological quality.

CRediT authorship contribution statement

Miriam Chiodetti: Validation, Formal analysis, Data curation, Writing – original draft, Visualization. **Maria Grazia Tuccio:** Conceptualization, Methodology, Validation, Investigation, Writing – review & editing. **Eleonora Carini:** Conceptualization, Methodology, Validation, Resources, Writing – review & editing, Supervision, Project administration, Funding acquisition.

Declaration of competing interest

The authors declare that they have no known competing financial interests or personal relationships that could have appeared to influence the work reported in this paper.

Data availability

Data will be made available on request.

Acknowledgements

The authors would like to thank Charles Bovary Nankouo for his contribution in data acquisition.

Appendix A. Supplementary data

Supplementary data to this article can be found online at https://doi.org/10.1016/j.crfs.2024.100780.

References

Abdel-Ghany, S.E., Ullah, F., Ben-Hur, A., Reddy, A.S.N., 2020. Transcriptome analysis of drought-resistant and drought-sensitive sorghum (Sorghum bicolor) genotypes in response to peg-induced drought stress. Int. J. Mol. Sci. 21, 1–26. https://doi.org/10.3390/ijms21030772.

Afify, A.E.M.M.R., El-Beltagi, H.S., El-Salam, S.M., Omran, A.A., 2012. Protein solubility, digestibility and fractionation after germination of sorghum varieties. PLoS One 7, 1–6. https://doi.org/10.1371/journal.pone.0031154.

Afify, A.E.M.M.R., El-Beltagi, H.S., El-Salam, S.M.A., Omran, A.A., 2011. Bioavailability of iron, zinc, phytate and phytase activity during soaking and germination of white sorghum varieties. PLoS One 6, 1–7. https://doi.org/10.1371/journal.pone.0025512.

Assifaoui, A., Champion, D., Chiotelli, E., Verel, A., 2006. Characterization of water mobility in biscuit dough using a low-field 1H NMR technique. Carbohydr. Polym. 64, 197–204. https://doi.org/10.1016/j.carbpol.2005.11.020.

Bean, S.R., Wilson, J.D., Moreau, R.A., Galant, A., Awika, J.M., Kaufman, R.C., Adrianos, S.L., Ioerger, B.P., 2019. Structure and composition of the sorghum grain. Sorghum State Art Futur. Perspect. 173–214. https://doi.org/10.2134/agronmonogr58.c9.

Belton, P.S., Taylor, J.R.N., 2004. Sorghum and millets: protein sources for Africa. Trends Food Sci. Technol. 15, 94–98. https://doi.org/10.1016/j.tifs.2003.09.002.

Borgia, G.C., Brown, R.J.S., Fantazzini, P., 1998. Uniform-penalty Inversion of Multiexponential decay data. J. Magn. Reson. 132, 65–77. https://doi.org/10.1006/jmre.1998.1387.

Borgia, G.C., Brown, R.J.S., Fantazzini, P., 2000. Uniform-penalty Inversion of Multiexponential decay data: II. Data spacing, T2 data, Systematic data Errors, and Diagnostics. J. Magn. Reson. 147, 273–285. https://doi.org/10.1006/jmre.2000.2197.

Bosmans, G.M., Lagrain, B., Deleu, L.J., Fierens, E., Hills, B.P., Delcour, J.A., 2012. Assignments of proton populations in dough and bread using NMR relaxometry of starch, gluten, and flour model systems. J. Agric. Food Chem. 60, 5461–5470. https://doi.org/10.1021/jf3008508.

Cardone, G., Rumler, R., Speranza, S., Marti, A., Schönlechner, R., 2021. Sprouting time affects sorghum (Sorghum bicolor [L.] moench) functionality and bread-baking performance. Foods 10, 1–17. https://doi.org/10.3390/foods10102285.

Ciacci, C., Maiuri, L., Caporaso, N., Bucci, C., Del Giudice, L., Rita Massardo, D., Pontieri, P., Di Fonzo, N., Bean, S.R., Ioerger, B., Londei, M., 2007. Celiac disease: in vitro and in vivo safety and palatability of wheat-free sorghum food products. Clin. Nutr. 26, 799–805. https://doi.org/10.1016/j.clnu.2007.05.006.

de Mesa-Stonestreet, N.J., Alavi, S., Bean, S.R., 2010. Sorghum proteins: the concentration, isolation, modification, and food applications of kafirins. J. Food Sci. 75 https://doi.org/10.1111/j.1750-3841.2010.01623.x.

de Morais Cardoso, L., Pinheiro, S.S., Martino, H.S.D., Pinheiro-Sant'Ana, H.M., 2017. Sorghum (Sorghum bicolor L.): Nutrients, bioactive compounds, and potential impact on human health. Crit. Rev. Food Sci. Nutr. 57, 372–390. https://doi.org/10.1080/10408398.2014.887057.

Dicko, M.H., Gruppen, H., Traoré, A.S., Voragen, A.G.J., Van Berkel, W.J.H., 2006. Sorghum grain as human food in Africa: relevance of content of starch and amylase activities. Afr. J. Biotechnol. 5, 384–395.

Donmez, D., Pinho, L., Patel, B., Desam, P., Campanella, O.H., 2021. Characterization of starch–water interactions and their effects on two key functional properties: starch gelatinization and retrogradation. Curr. Opin. Food Sci. 39, 103–109. https://doi.org/10.1016/j.cofs.2020.12.018.

Elkhalifa, A.E.O., Bernhardt, R., 2010. Influence of grain germination on functional properties of sorghum flour. Food Chem. 121, 387–392. https://doi.org/10.1016/j.foodchem.2009.12.041.

Elkhalifa, A.E.O., Bernhardt, R., 2013. Some physicochemical properties of flour from germinated sorghum grain. J. Food Sci. Technol. 50, 186–190. https://doi.org/10.1007/s13197-011-0315-2.

Espitia-Hernández, P., Chávez González, M.L., Ascacio-Valdés, J.A., Dávila-Medina, D., Flores-Naveda, A., Silva, T., Ruelas Chacón, X., Sepúlveda, L., 2022. Sorghum (Sorghum bicolor L.) as a potential source of bioactive substances and their biological properties. Crit. Rev. Food Sci. Nutr. 62, 2269–2280. https://doi.org/10.1080/10408398.2020.1852389.

FAOSTAT, 2021. Crops and Livestock products. Retrieved from. https://www.fao.org/faostat/en/#data/QCL. (Accessed 8 January 2024).

Fu, Z.Q., Wang, L.J., Zou, H., Li, D., Adhikari, B., 2014. Studies on the starch-water interactions between partially gelatinized corn starch and water during gelatinization. Carbohydr. Polym. 101, 727–732. https://doi.org/10.1016/j.carbpol.2013.09.098.

Georget, D.M.R., Elkhalifa, A.E.O., Peter, S.B., 2012. Structural changes in kafirin extracted from a white type II tannin sorghum during germination. J. Cereal. Sci. 55, 106–111. https://doi.org/10.1016/j.jcs.2011.10.007.

Goldstein, A., Nantanga, K.K.M., Seetharaman, K., 2010. Molecular interactions in starch-water systems: effect of increasing starch concentration. Cereal Chem. 87, 370–375. https://doi.org/10.1094/CCHEM-87-4-0370.

Hager, A.S., Bosmans, G.M., Delcour, J.A., 2014. Physical and molecular changes during the storage of gluten-free rice and oat bread. J. Agric. Food Chem. 62, 5682–5689. https://doi.org/10.1021/jf502036x.

Hariprasanna, K., Rakshit, S., 2016. Economic Importance of Sorghum 1–25. https://doi.org/10.1007/978-3-319-47789-3_1.

Jakobi, S., Jekle, M., Becker, T., 2018. Direct link between specific structural levels of starch and hydration properties. Carbohydr. Polym. 181, 159–166. https://doi.org/10.1016/j.carbpol.2017.10.062.

Khoddami, A., Messina, V., Vadabalija Venkata, K., Farahnaky, A., Blanchard, C.L., Roberts, T.H., 2023. Sorghum in foods: functionality and potential in innovative products. Crit. Rev. Food Sci. Nutr. 63, 1170–1186. https://doi.org/10.1080/10408398.2021.1960793.

Le Botlan, D., Rugraff, Y., Martin, C., Colonna, P., 1998. Quantitative determination of bound water in wheat starch by time domain NMR spectroscopy. Carbohydr. Res. 308, 29–36. https://doi.org/10.1016/S0008-6215(98)00068-8.

Le Grand, F., Cambert, M., Mariette, F., 2007. NMR signal analysis to characterize solid, aqueous, and lipid phases in baked cakes. J. Agric. Food Chem. 55, 10947–10952. https://doi.org/10.1021/jf071735r.

Lemmens, E., Moroni, A.V., Pagand, J., Heirbaut, P., Ritala, A., Karlen, Y., Kim-Anne, L., Van den Broeck, H.C., Brouns, F.J.P.H., De Brier, N., Delcour, J.A., 2019. Impact of cereal seed sprouting on its nutritional and technological properties: a Critical review. Compr. Rev. Food Sci. Food Saf. 18, 305–328. https://doi.org/10.1111/1541-4337.12414.

Li, C., Oh, S.G., Lee, D.H., Baik, H.W., Chung, H.J., 2017. Effect of germination on the structures and physicochemical properties of starches from brown rice, oat, sorghum, and millet. Int. J. Biol. Macromol. 105, 931–939. https://doi.org/10.1016/j.ijbiomac.2017.07.123.

Li, J.Y., Yeh, A.I., 2001. Relationships between thermal, rheological characteristics and swelling power for various starches. J. Food Eng. 50, 141–148. https://doi.org/10.1016/S0260-8774(00)00236-3.

Lin, L., Cai, C., Gilbert, R.G., Li, E., Wang, J., Wei, C., 2016. Relationships between amylopectin molecular structures andfunctional properties of different-sized fractions of normal andhigh-amylose maize starches. Food Hydrocolloids 52, 359–368. https://doi.org/10.1016/j.foodhyd.2015.07.019.

Liu, Q., Yada, R., Arul, J., 2002. Characterization of thermal properties of potato dry matter - water and starch - water systems. J. Food Sci. 67, 560–566. https://doi.org/10.1111/j.1365-2621.2002.tb10638.x.
Marchini, M., Arduini, R., Carini, E., 2021a. Insight into molecular and rheological properties of sprouted sorghum flour. Food Chem. 356, 129603 https://doi.org/10.1016/j.foodchem.2021.129603.
Marchini, M., Marti, A., Folli, C., Prandi, B., Ganino, T., Conte, P., Fadda, C., Mattarozzi, M., Carini, E., 2021b. Sprouting of sorghum (Sorghum bicolor [l.] moench): effect of drying treatment on protein and starch features. Foods 10, 1–17. https://doi.org/10.3390/foods10020407.
Marchini, M., Paciulli, M., Broccardo, L., Tuccio, M.G., Scazzina, F., Cirlini, M., Carini, E., 2023. Towards Sustainable and nutritionally Enhanced Flatbreads from sprouted sorghum, tapioca, and Cowpea climate-resilient crops. Foods 12. https://doi.org/10.3390/foods12081638.
Marengo, M., Carpen, A., Bonomi, F., Casiraghi, M.C., Meroni, E., Quaglia, L., Iametti, S., Pagani, M.A., Marti, A., 2017. Macromolecular and micronutrient profiles of sprouted chickpeas to be used for integrating cereal-based food. Cereal Chem. 94, 82–88. https://doi.org/10.1094/CCHEM-04-16-0108-FI.
Marti, A., Cardone, G., Nicolodi, A., Quaglia, L., Pagani, M.A., 2017. Sprouted wheat as an alternative to conventional flour improvers in bread-making. Lwt 80, 230–236. https://doi.org/10.1016/j.lwt.2017.02.028.
Meiboom, S., Gill, D., 1958. Modified spin-echo method for measuring nuclear relaxation times. Rev. Sci. Instrum. 29, 688–691. https://doi.org/10.1063/1.1716296.
Orlowska, M., Randzio, S.L., 2010. Water content influence on thermal and volumetric properties of wheat starch gelatinization under 10 MPa. Ann. N. Y. Acad. Sci. 1189, 43–54. https://doi.org/10.1111/j.1749-6632.2009.05205.x.
Parenti, O., Guerrini, L., Zanoni, B., Marchini, M., Tuccio, M.G., Carini, E., 2021. Use of the 1H NMR technique to describe the kneading step of wholewheat dough: the effect of kneading time and total water content. Food Chem. 338, 128120 https://doi.org/10.1016/j.foodchem.2020.128120.
Pontieri, P., Mamone, G., De Caro, S., Tuinstra, M.R., Roemer, E., Okot, J., De Vita, P., Ficco, D.B.M., Alifano, P., Pignone, D., Massardo, D.R., Del Giudice, L., 2013. Sorghum, a healthy and gluten-free food for celiac patients as demonstrated by genome, biochemical, and immunochemical analyses. J. Agric. Food Chem. 61, 2565–2571. https://doi.org/10.1021/jf304882k.
Rakhshi, E., Cambert, M., Diascorn, Y., Lucas, T., Rondeau-Mouro, C., 2022. An insight into tapioca and wheat starch gelatinization mechanisms using TD-NMR and complementary techniques. Magn. Reson. Chem. 60, 702–718. https://doi.org/10.1002/mrc.5258.
Rakhshi, E., Falourd, X., Adel, R. den, van Duynhoven, J., Lucas, T., Rondeau-Mouro, C., 2024. Multi-scale investigation of the heat-induced transformation of starch in model dough and starch systems. Food Hydrocolloids 149, 109616. https://doi.org/10.1016/j.foodhyd.2023.109616.
Rashwan, A.K., Yones, H.A., Karim, N., Taha, E.M., Chen, W., 2021. Potential processing technologies for developing sorghum-based food products: an update and comprehensive review. Trends Food Sci. Technol. 110, 168–182. https://doi.org/10.1016/j.tifs.2021.01.087.
Riley, I.M., Nivelle, M.A., Ooms, N., Delcour, J.A., 2022. The use of time domain 1H NMR to study proton dynamics in starch-rich foods: a review. Compr. Rev. Food Sci. Food Saf. 21, 4738–4775. https://doi.org/10.1111/1541-4337.13029.
Rondeau-Mouro, C., Cambert, M., Kovrlija, R., Musse, M., Lucas, T., Mariette, F., 2015. Temperature-associated proton dynamics in wheat starch-based model systems and wheat flour dough evaluated by NMR. Food Bioprocess Technol. 8, 777–790. https://doi.org/10.1007/s11947-014-1445-0.
Ruan, R.R., Wang, X., Chen, P.L., Fulcher, R.G., Pesheck, P., Chakrabarti, S., 1999. Study of water in dough using nuclear magnetic resonance. Cereal Chem. 76, 231–235. https://doi.org/10.1094/cchem.1999.76.2.231.
Rumler, R., Bender, D., Schönlechner, R., 2022. Sorghum and its potential for the Western diet, 0–3 J. Cereal. Sci. 104. https://doi.org/10.1016/j.jcs.2022.103425.
Rumler, R., Schönlechner, R., 2021. Effect of sorghum on rheology and final quality of western style breads: a literature review. Foods 10, 1392. https://doi.org/10.3390/foods10061392.
Saithalavi, K.M., Bhasin, A., Yaqoob, M., 2021. Impact of sprouting on physicochemical and nutritional properties of sorghum: a review. J. Food Meas. Char. 15, 4190–4204. https://doi.org/10.1007/s11694-021-00969-9.
Schirmer, M., Jekle, M., Becker, T., 2015. Starch gelatinization and its complexity for analysis. Starch/Staerke 67, 30–41. https://doi.org/10.1002/star.201400071.
Serna-Saldivar, S.O., Espinosa-Ramírez, J., 2019. Grain structure and grain chemical composition. In: Sorghum and Millets. Elsevier, pp. 85–129. https://doi.org/10.1016/B978-0-12-811527-5.00005-8.
Singh, A., Sharma, S., Singh, B., 2017. Effect of germination time and temperature on the functionality and protein solubility of sorghum flour. J. Cereal. Sci. 76, 131–139. https://doi.org/10.1016/j.jcs.2017.06.003.
Tananuwong, K., Reid, D.S., 2004. DSC and NMR relaxation studies of starch-water interactions during gelatinization. Carbohydr. Polym. 58, 345–358. https://doi.org/10.1016/j.carbpol.2004.08.003.
Taylor, J.R.N., Schober, T.J., Bean, S.R., 2006. Novel food and non-food uses for sorghum and millets. J. Cereal. Sci. 44, 252–271. https://doi.org/10.1016/j.jcs.2006.06.009.
Vanamala, J.K.P., Massey, A.R., Pinnamaneni, S.R., Reddivari, L., Reardon, K.F., 2018. Grain and sweet sorghum (Sorghum bicolor L. Moench) serves as a novel source of bioactive compounds for human health. Crit. Rev. Food Sci. Nutr. 58, 2867–2881. https://doi.org/10.1080/10408398.2017.1344186.
Wang, S., Copeland, L., 2012. Phase transitions of pea starch over a wide range of water content. J. Agric. Food Chem. 60, 6439–6446. https://doi.org/10.1021/jf3011992.
Wang, S., Copeland, L., 2013. Molecular disassembly of starch granules during gelatinization and its effect on starch digestibility: a review. Food Funct. 4, 1564–1580. https://doi.org/10.1039/c3fo60258c.
Wang, S., Li, C., Yu, J., Copeland, L., Wang, S., 2014. Phase transition and swelling behaviour of different starch granules over a wide range of water content. Lwt 59, 597–604. https://doi.org/10.1016/j.lwt.2014.06.028.
Wu, F., Chen, H., Yang, N., Wang, J., Duan, X., Jin, Z., Xu, X., 2013. Effect of germination time on physicochemical properties of brown rice flour and starch from different rice cultivars. J. Cereal. Sci. 58, 263–271. https://doi.org/10.1016/j.jcs.2013.06.008.
Xiong, Y., Zhang, P., Warner, R.D., Fang, Z., 2019. Sorghum grain: from Genotype, nutrition, and phenolic profile to its health benefits and food applications. Compr. Rev. Food Sci. Food Saf. 18, 2025–2046. https://doi.org/10.1111/1541-4337.12506.
Zhang, Z., Li, E., Fan, X., Yang, C., Ma, H., Gilbert, R.G., 2020. The effects of the chain-length distributions of starch molecules on rheological and thermal properties of wheat flour paste. Food Hydrocolloids 101, 105563. https://doi.org/10.1016/j.foodhyd.2019.105563.
Zhu, F., 2014. Structure, physicochemical properties, modifications, and uses of sorghum starch. Compr. Rev. Food Sci. Food Saf. 13, 597–610. https://doi.org/10.1111/1541-4337.12070.